THE JOURNAL OF BIOLOGICAL CHEMISTRY VOL. 284, NO. 15, pp. 9955–9964, April 10, 2009

Counteracting Signaling Activities in Lipid Rafts Associated with the Invasion of Lung Epithelial Cells by *Pseudomonas aeruginosa*[*]

Received for publication, November 13, 2008, and in revised form, February 5, 2009 Published, JBC Papers in Press, February 11, 2009, DOI 10.1074/jbc.M808629200

David W. Zaas[‡1], Zachary D. Swan[‡], Bethany J. Brown[§], Guojie Li[¶], Scott H. Randell[‖], Simone Degan[**], Mary E. Sunday[**], Jo Rae Wright[§], and Soman N. Abraham[¶‡‡]**

From the [‡]Division of Pulmonary, Allergy, and Critical Care Medicine, Department of Medicine, and Departments of [§]Cell Biology, [¶]Pathology, [**]Immunology, and [‡‡]Molecular Genetics and Microbiology, Duke University Medical Center, Durham, North Carolina 27710 and the [‖]Departments of Cell and Molecular Physiology and Medicine, University of North Carolina, Chapel Hill, North Carolina 27599

Pseudomonas aeruginosa **has the capacity to invade lung epithelial cells by co-opting the intrinsic endocytic properties of lipid rafts, which are rich in cholesterol, sphingolipids, and proteins, such as caveolin-1 and -2. We compared intratracheal *Pseudomonas* infection in wild type and caveolin-deficient mice to investigate the role of caveolin proteins in the pathogenesis of *Pseudomonas* pneumonia. Unlike wild type mice, which succumb to pneumonia, caveolin-deficient mice are resistant to *Pseudomonas*. We observed that *Pseudomonas* invasion of lung epithelial cells is dependent on caveolin-2 but not caveolin-1. Phosphorylation of caveolin-2 by Src family kinases is an essential event for *Pseudomonas* invasion. Our studies also reveal the existence of a distinct signaling mechanism in lung epithelial cells mediated by COOH-terminal Src kinase (Csk) that negatively regulates *Pseudomonas* invasion. Csk migrates to lipid raft domains, where it decreases phosphorylation of caveolin-2 by inactivating c-Src. Whereas *Pseudomonas* co-opts the endocytic properties of caveolin-2 for invasion, there also exists in these cells an intrinsic Csk-dependent cellular defense mechanism aimed at impairing this activity. The success of *Pseudomonas* in co-opting lipid raft-mediated endocytosis to invade lung epithelial cells may depend on the relative strengths of these counteracting signaling activities.**

Pseudomonas (Pa)[2] is an important cause of hospital-acquired and healthcare-associated pneumonia (1–4). Despite appropriate antibiotic therapy, the morbidity and mortality associated with Pa pneumonia remains high, at least partly due to the ability of Pa to resist antibiotic-mediated killing (1, 5). It has recently been recognized that Pa is not solely an extracellular pathogen and that Pa can invade lung epithelial cells (LECs) via lipid raft-mediated endocytosis (6–8). Lipid rafts are specialized areas of the plasma membrane that are detergent-insoluble, low density membrane fractions enriched in cholesterol and sphingolipids (9). An increasing number of pathogens have been recognized to co-opt the mechanism of lipid raft-mediated endocytosis in order to invade host cells (10–12). We have previously shown that Pa co-opts the host endocytic machinery to invade both LECs where it can survive and replicate (6).

The uptake of Pa requires the expression of several lipid raft-associated proteins, including the caveolin proteins (6). Caveolin-1 and -2 are co-expressed on a wide range of cell types but are particularly abundant in endothelial cells, airway epithelial cells, and type I pneumocytes (9, 13, 14). Caveolin-1 has been implicated as a scaffolding protein for organizing and concentrating caveolin-interacting signaling molecules within caveolae. Caveolin-2 is the most divergent of the caveolin gene family, with only ~50% similarity to caveolin-1 (15). Caveolin-2 interacts with caveolin-1 to form a hetero-oligomeric complex within lipid rafts (14). In order for caveolin-2 to be expressed, caveolin-1 serves as a chaperone to transport caveolin-2 to the plasma membrane. In the absence of caveolin-1, caveolin-2 is degraded in the Golgi apparatus, and no significant caveolin-2 is expressed (14). As expected based on these observations, the caveolin-1 knock-out mouse lacks expression of both caveolin-1 and -2 and is functionally deficient in both caveolin-1 and -2 (16). In addition to serving as key structural proteins that organize caveolae platforms, caveolin proteins are important in regulating endocytosis and cell signaling (17, 18). Caveolin proteins serve to regulate cell signaling pathways that are concentrated within lipid rafts and have recognized sites of tyrosine phosphorylation that interact with members of the Src family kinases (19–22). Studies of the caveolin knock-out mouse have shown that caveolin plays important roles within the lung (16, 23, 24); however, the role of caveolin proteins and lipid raft-mediated uptake in the pathogenesis of Pa pneumonia is not well understood.

The primary aim of this study is to investigate the role of caveolin proteins in the pathogenesis of Pa pneumonia. We have hypothesized that Pa invasion of LECs is an important virulence factor for Pa in the pathogenesis of pneumonia. The ability of Pa to invade LECs allows for a protected intracellular niche where Pa may be able to replicate and avoid innate host defense mechanisms. In this study, we show that caveolin-defi-

* This work was supported, in whole or in part, by National Institutes of Health Grants HL083092 (to D. W. Z.), HL084917 (to M. S.), HL-30923 (to J. R. W.), DK050814-28 (to S. N. A.), and DK065988 (for mouse tracheal epithelial cell culture) (to S. H. R.). This research was also supported by the Parker B. Francis Foundation.

[1] To whom correspondence should be addressed: Division of Pulmonary, Allergy and Critical Care Medicine, Dept. of Medicine, Duke University, DUMC Box 3501, Bell Bldg., Rm. 350, Durham, NC 27710. Tel.: 919-684-2728; Fax: 919-684-3067; E-mail: david.zaas@duke.edu.

[2] The abbreviations used are: Pa, *Pseudomonas*; LEC, lung epithelial cell; cav, caveolin; Csk, COOH-terminal Src kinase; MCD, methyl-β-cyclodextrin; MLE-12, murine lung epithelial cell line-12; GFP, green fluorescent protein; cfu, colony-forming unit; BAL, bronchoalveolar lavage; PBS, phosphate-buffered saline.

cient mice are less susceptible to Pa pneumonia due to the inability of Pa to invade LECs. The lipid raft-mediated uptake of Pa requires the phosphorylation of caveolin-2 by the Src family of tyrosine kinases. Surprisingly, we also observed that knocking down of the COOH-terminal Src kinase (Csk) resulted in a 4-fold increase in the invasion of Pa into LECs, revealing the existence of a host cell-mediated response directed at limiting invasion of Pa. Following exposure to Pa, Csk was found to migrate to lipid raft fractions of LECs and to inhibit phosphorylation of caveolin-2. The importance of Csk in negatively regulating caveolin-2 and lipid raft-mediated Pa uptake may provide valuable clues for the development of novel therapies aimed at abrogating Pa pneumonia in high risk patients.

EXPERIMENTAL PROCEDURES

Animals—Breeding pairs of caveolin-1 knock-out ($cav^{-/-}$) mice (*Cav*^{tm1Mls}/J) and control ($cav^{+/+}$) mice (*B6129SF2/J*) were obtained from Jackson Laboratory. Mice were housed and bred in pathogen-free facilities at Duke University and handled according to approved IACUC protocols.

Bacterial Strains and Cell Lines—Pseudomonas aeruginosa strain 27853, and PAO-1 were obtained from the American Type Culture Collection (Manassas, VA). Strain S4270 is a clinical isolate that was obtained from the Duke clinical microbiology laboratory. *P. aeruginosa* strains were grown in 5 ml of static LB broth for 18 h. *Staphylococcus aureus* was grown for 18 h in 5 ml of brain heart infusion broth (BD Biosciences). After static incubation for 18 h, bacterial cultures were diluted 1:50 and placed on a shaker at 37 °C for 2–3 h until they reached midlog growth phase with an A_{600} of 0.4–0.8. GFP-expressing strains of Pa were created using pSMC2-GFP vector provided by George O'Toole (Dartmouth) (25). Pa was made competent using a magnesium competency protocol and were transfected with the pSMC2-GFP vector (26).

Murine Model of Pa Pneumonia—The $cav^{-/-}$ and $cav^{+/+}$ mice were infected with bacteria via direct transtracheal instillation. Mice were sedated with ketamine and xylizine, and a surgical incision was made in the neck to directly expose the trachea. Approximately 10^7 cfu of Pa (ATCC 27853) diluted in 50 μl of Hanks' buffered saline solution was instilled into the trachea via a 30-gauge needle. The incision was closed with a suture, and the mice were monitored over the next 10 days. Any mice that were moribund were sacrificed using CO_2 inhalation. A total 7 mice/group were used for each of the three experimental replicates that were performed for the survival analysis. For secondary endpoints, mice were sacrificed at 16 h by a lethal overdose of pentobarbital. Bronchoalveolar lavage (BAL) was performed with three serial 1-ml lavages. The lung was removed and fixed in formalin for histological analysis. Additional lung tissue was homogenized in sterile PBS, and serial dilutions were plated to obtain data on bacterial burden measured by colony forming units. Quantitative analysis was carried out to determine the relative extent of lung consolidation by pneumonia. The lungs were all inflated to a constant pressure of 25 mm Hg. The area of lung tissue was calculated out using ImageJ software (version 1.40g). For each slide (representing one mouse), seven nonoverlapping images were taken randomly at ×20 magnification. The total alveolar tissue area was determined using thresholding, and the final volume of the tissue in all seven fields was averaged. The data were expressed as mean percentage of the total field ± S.E. The final volume of the tissue in all seven fields was averaged, and the data were expressed as mean percentage of the total field ± S.E.

Isolation of Primary Cells—Murine tracheal epithelial cells from both $cav^{+/+}$ and $cav^{-/-}$ were isolated as described previously (27, 28) and were grown on transwells with an air-liquid interface. In addition, primary alveolar macrophages were isolated according to our previously published protocols (29). Cytospins of lavages stained with the Hemacolor stain kit revealed macrophage populations greater than 95% of total cells. The isolated primary cells were then infected with 10^5 cfu of Pa ATCC 27853 diluted in 100 μl of serum-free medium. A gentamicin protection assay was performed as described below to quantify the number of intracellular bacteria within the primary tracheal epithelial cells and alveolar macrophages.

Cell Lines and Constructs—The murine lung epithelial cell line, MLE-12, was graciously provided by Landon King (The Johns Hopkins University) and was grown in RPMI 1640 (Invitrogen) supplemented with 10% fetal bovine serum (Hyclone), 2.0 g/liter sodium bicarbonate, 0.3 g/liter L-glutamine, 2.5 g/liter glucose, 10 mM HEPES, and 1 mM sodium pyruvate. RNA interference vectors were generated using pQCXIN retroviral vector (BD Biosciences). Briefly, pQCXIN was digested by BamHI and EcoRI and then was ligated to generate pQCXIN1. Human U6 small nuclear RNA promoter was PCR-amplified from pTZ U6 + 1 (a gift from John Rossi, Beckman Research Institute of the City of Hope, Duarte, CA) with an added BglII site (5′-ends) and BamHI and XbaI sites (3′-ends). The following oligonucleotides were ordered from Integrated DNA Technologies, Inc. (Coralville, IA): 5′-GAT CCG CTG AGC ATT GAT GAG GAG TTC AAG AGA CTC CTC ATC AAT GCT CAGC TTT TTT-3′ and 5′-CTA GAA AAA AGC TGA GCA TTG ATG AGG AGT CTC TTG AAC TCC TCA ATG CTC AGC G-3′ to generate pQC-Csk. Control vectors were created using a nonsense sequence to create the pQC-LUC cell line as a control. 5′-GAT CCG TAC GCG GAA TAC TTC GAA TTC AAG AGA TTC GAA GTA TTC CGC GTA CTT TTT T-3′ and 5′-CTA GAA AAA AGT ACG CGG AAT ACT TCG AAT CTC TTG AAT TCG AAG TAT TCC GCG TAC G-3′ correspond to nucleotides 423–441 of the firefly luciferase in the pGL2-control vector. GenBank™ accession number X65324 was used to generate the control cell line pQC-LUC. The Amphopack-293 cell line (BD Biosciences) was used to produce the viral particles.

The 3×FLAG fragment from p3×FLAg-CMV-10 (Sigma) was PCR-amplified using FLAGF (5′-CCG GGA TCC ACG GGC TGA CTA CAA AGA CCA TGA CGG TGA T-3′) and FLAGR (5′-TTC GCG GCC GCT CAC TAC TTG TCA TCG TCA TCC TTG TA-3′). pLEGFP-N1 (Clontech) was then ligated with the 3×FLAG fragment to generate pFLAG-N1. The caveolin-1 gene was PCR-amplified using Cav1F (5′-GAT CTC GAG ATG TCT GGG GGC AAA TAC GT-3′) and Cav1R (5′-GAT GGA TCC CGT ATC TCT TTC TGC GTG CTG ATG-3′) to generate pCav1-FLAG. The caveolin-2 gene was PCR-amplified using 2F (5′-CTC AGA TCT CAT GGG GCT GGA GAC CGA GAA G-3′) and Cav2R (5′-GAT AAG CTT

GTC GTG GCT CAG TTG CAT GCT-3′) to generate pCav2-FLAG. All constructs were sequenced to confirm sequence accuracy and in-frame of translation.

Gentamicin Protection Assays—MLE-12 cells were grown to ~80% confluence for all experiments. For infections with strains of *P. aeruginosa*, cells were infected at a multiplicity of infection of 300–600 bacteria/host cell by the addition of 100 μl of bacteria diluted in serum-free cell culture medium containing 10 mg/ml bovine serum albumin (Sigma). Plates were then incubated at 37 °C for 60 min. The medium was replaced with fresh culture medium containing 50 μg/ml of the membrane-impermeable antibiotic gentamicin (Invitrogen) to kill extracellular bacteria and incubated for 45 min. Each well was washed three times with PBS. In order to remove and lyse the cells, 30 μl of 0.25% trypsin (Invitrogen) was added to each well for 5 min, and 70 μl of 0.1% Triton X-100 in PBS was then added. Cells were scraped and transferred to 0.65-ml tubes, and each well was washed with an additional 100 μl of Triton that was also transferred to the tubes. The cell lysates were diluted and plated onto agar plates where colonies were counted to quantify the number of intracellular bacteria. To test the effect of pretreatment by specific lipid raft disrupters/usurpers on bacterial invasion, methyl-β-cyclodextrin (MCD; 3 mM; Sigma) in serum-free medium was added to the cells for 30 min and then washed off prior to infection. To test the effect of altering tyrosine phosphorylation on bacterial invasion, the cells were pretreated with genistein (100 μg/ml; Sigma) for 30 min prior to infection and throughout the period of infection. After the preincubation step, the cells were washed, and the medium was replaced with bacteria in serum-free medium with or without the agent being tested as required. The data shown represent a combination of three separate experiments for each of the bacterial invasion studies. The viability of the cells was not affected by any of the drug treatments used as determined by trypan blue exclusion.

Confocal Microscopy—MLE-12 cells were seeded onto collagen-coated 12-mm diameter glass coverslips placed into the wells of a 24-well plate and grown for 36 h. The cells were infected with ATCC 27853 strain of *P. aeruginosa* expressing GFP (25). The infected cells were incubated at 37 °C for 60 min, washed four times with PBS (Invitrogen) to remove unbound bacteria, and fixed overnight in 2.0% paraformaldehyde in PBS. After removing the fixative, the cells were permeabilized with 0.1% Triton X-100 (Sigma). Csk was then labeled using polyclonal anti-Csk antibody (Upstate Biotechnology, Inc.) and Alexa-fluor 660 secondary antibodies (Molecular Probes). Frozen sections of murine lungs infected with GFP-expressing Pa were also examined with a confocal microscopy to identify the localization of Pa infection *in vivo*. Lung sections were fixed with 1% paraformaldehyde and stained with CellMask deep red plasma membrane stain (Invitrogen). Coverslips were examined using a Nikon Eclipse TE200 microscope.

Western Blotting and Immunoprecipitation—The following antibodies were used: anti-rabbit polyclonal caveolin-2 (Abcam), anti-mouse monoclonal caveolin-2 (BD Biosciences), anti-mouse monoclonal FLAG antibody (Sigma), anti-rabbit polyclonal Csk (BD Biosciences), anti-mouse Csk (BD Biosciences), anti-rabbit c-Src (eBiosciences), anti-mouse c-Src clone GD11 (Upstate Biotechnology), anti-rabbit src529PY (BIOSOURCE), and anti-rabbit tyrosine phosphorylation (BD Biosciences).

Cells were grown in a 6-well plate to greater than 90% confluence. Cells were lysed with lysis buffer (1:10; Upstate Biotechnology), phenylmethylsulfonyl fluoride (1 mM), and protease inhibitor mixture (1:100; Sigma). Cell lysates were normalized for protein and volume. Samples were diluted in Laemmli sample buffer (Bio-Rad) with mercaptoethanol and boiled for 5 min. Proteins were resolved by SDS-PAGE and transferred to nitrocellulose membranes. The proteins were detected using the Super Signal West Pico chemiluminescent kit (Pierce).

Csk, c-Src, and FLAG-caveolin-2 were immunoprecipitated from whole cell lysates of MLE-12 cells as follows. MLE-12 cells were grown to 90% confluence in 6-well plates. The cells were washed twice with cold PBS. The cells were then lysed in 500 μl of lysis buffer (lysis buffer (Upstate Biotechnology; 1:10), *n*-octyl-β-D-glucopyranoside (60 mM; Sigma), phenylmethylsulfonyl fluoride (1 mM), protease inhibitor, phosphatase mixture (Sigma; 1:100)). The sample was precleared with 30 μl of a 50% suspension of protein G-Sepharose (Sigma) in PBS for 1 h at 4 °C. The samples were then incubated for 16 h at 4 °C with 50 μl of a 50% suspension of protein G-Sepharose in PBS plus the indicated primary antibodies. The immunoprecipitates were washed three times with 1 ml of PBS and resuspended in 50 μl of Laemmli sample buffer (Bio-Rad) with mercaptoethanol and boiled for 5 min. Immunoprecipitates were assayed by Western blotting as described above, and all experimental results were replicated in at least three separate experiments.

Statistics—Data were compiled and analyzed using Microsoft Excel® and Graphpad® Prism software. Data for gentamicin protection assays are reported as a mean of at least three experiments with error bars set as S.E. Significance was calculated using a two-tailed *t* test or analysis of variance for multiple comparisons with significance defined as a p value of less than 0.05 (indicated by *asterisks*). Survival curves were analyzed using Kaplan Meir survival curves and log rank test in Graph Pad® Prism 3.0.

RESULTS

Caveolin-deficient Mice ($cav^{-/-}$) Have Lower Mortality after Intratracheal Infection with Pa—Direct intratracheal instillation of Pa was selected as a murine model of acute bacterial pneumonia. Both caveolin-deficient ($cav^{-/-}$) and wild type ($cav^{+/+}$) strains of mice were infected with 10^7 cfu of Pa (ATCC strain 27853) via direct intratracheal instillation and observed over 10 days. The $cav^{+/+}$ rapidly succumbed to Pa pneumonia with 25% mortality within 24 h and 100% mortality by 48 h (Fig. 1*A*). In contrast, the $cav^{-/-}$ mice were profoundly resistant and showed significantly greater survival than $cav^{+/+}$ controls (hazard ratio 2.903, log rank p value <0.0001). None of the $cav^{-/-}$ mice had died during the first 24 h, and any deaths occurred later than $cav^{+/+}$ controls. The surviving mice were monitored over 10 days, and the remaining $cav^{-/-}$ mice not only survived but also fully cleared the bacterial infection. The surviving mice were sacrificed at day 10, and cultures of BAL and lung homogenates revealed no growth of Pa.

Lungs of cav$^{-/-}$ Mice Have Significantly Lower Bacterial Burden after Intratracheal Instillation of Pa—In order to analyze the early response to Pa pneumonia, both groups of mice were infected again with 10^7 cfu of Pa and sacrificed prior to any mortality at 16 h after infection. CFU analysis from mice sacrificed 30 min after infection confirmed that the same amount of bacteria was delivered to the lungs of both groups (data not shown). Mice underwent BAL as well as the removal of lungs, liver, and spleen to quantify bacterial burden. cav$^{-/-}$ mice had significantly lower levels of Pa in both the BAL fluid (Fig. 1*B*; $p = 0.0067$) and the lung tissue (Fig. 1*C*; $p = 0.0022$). Both groups of mice showed signs of systemic bacteremia with dissemination of Pa to the liver (Fig. 1*D*) and spleen (Fig. 1*E*), but there was no difference between the two groups.

cav$^{-/-}$ Mice Have Less Lung Injury and Lower Levels of Inflammatory Cytokines in the Response to Pa Infection—The BAL total cell counts with differentials and cytokine responses were compared after Pa infection or saline-instilled controls. At base line, we found no differences in the BAL cell counts or levels of inflammatory cytokines between cav$^{+/+}$ and cav$^{-/-}$ mice. The BAL cell counts in both cav$^{-/-}$ and cav$^{+/+}$ mice were >90% neutrophils at 16 h after Pa infection (data not shown). The cav$^{-/-}$ mice had lower total cell counts and a lower number of neutrophils compared with cav$^{+/+}$ mice (Fig. 1*F*; $p = 0.16$), revealing a trend toward a lower level inflammatory response. Cytokine measurements in BAL fluid also demonstrated lower levels of inflammation in the cav$^{-/-}$ mice compared with cav$^{+/+}$ controls. BAL fluid collected 16 h after Pa infection demonstrated that the cav$^{-/-}$ mice had significantly lower levels of MIP-2 (Fig. 1*G*; $p = 0.039$), IL-1β (Fig. 1*H*; $p = 0.0001$), and tumor necrosis factor-α (Fig. 1*I*; $p = 0.016$).

Base-line lung histology examined prior to infection showed no

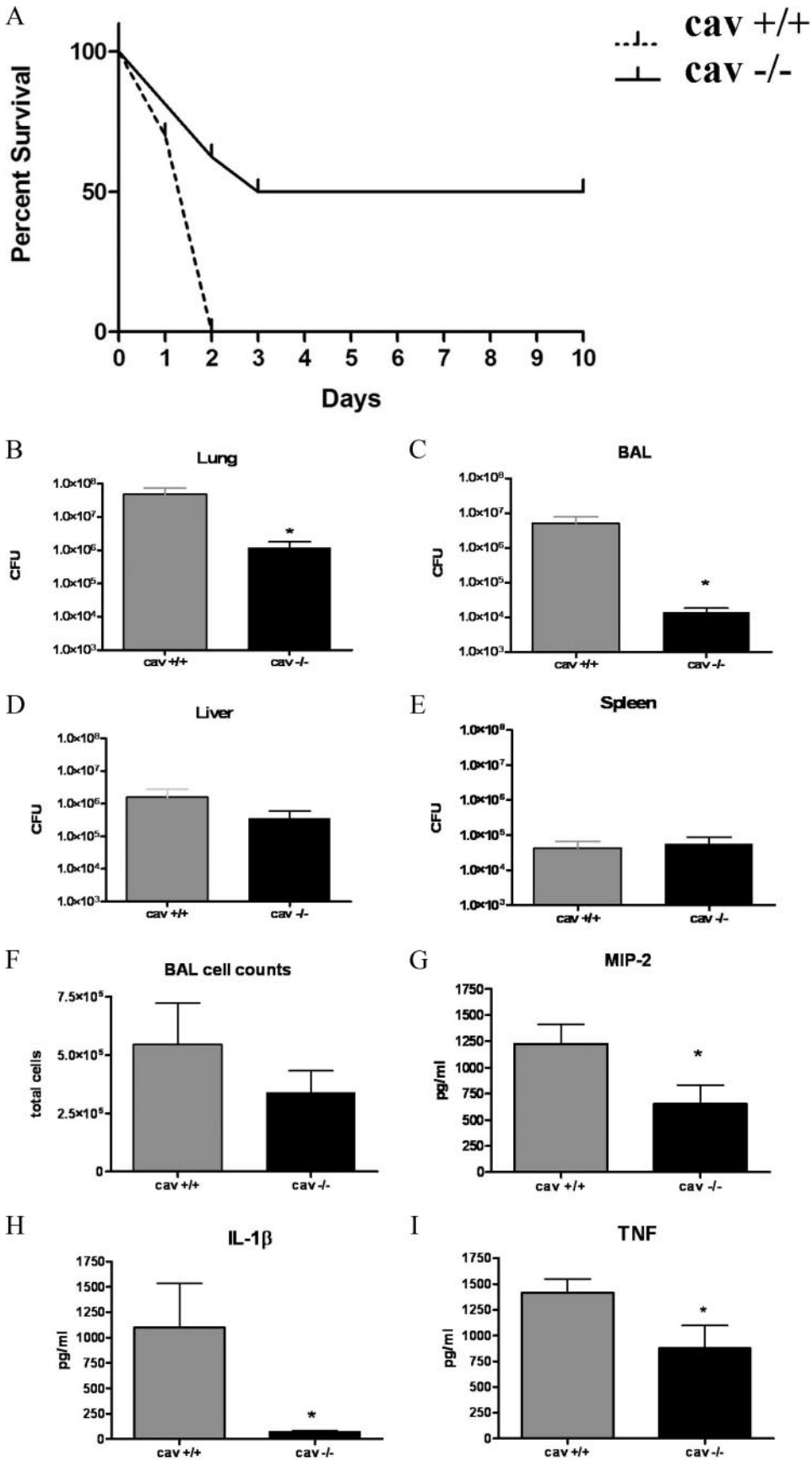

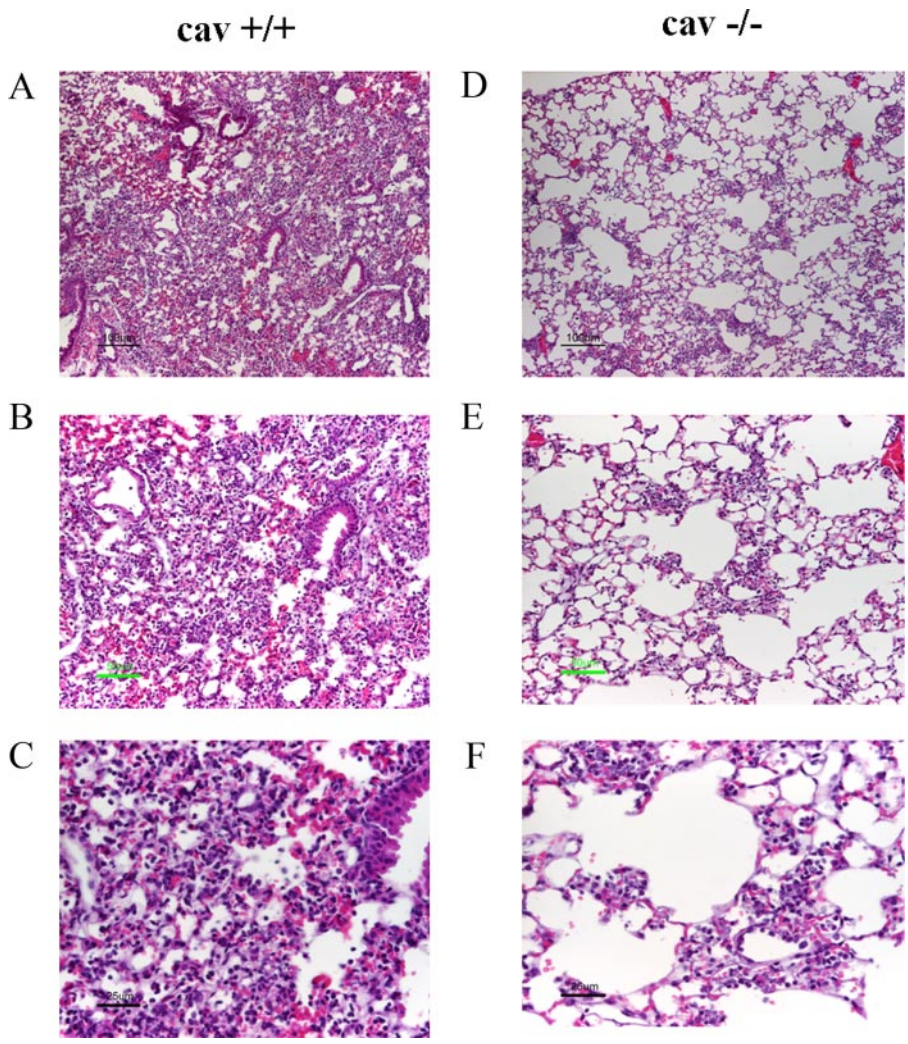

FIGURE 2. **cav$^{-/-}$ mice have diminished lung injury after Pa infection.** Lung histology was examined 16 h after infection. The lungs of cav$^{+/+}$ mice (*A–C*) are severely consolidated, with little evidence of remaining air spaces for gas exchange, evident at ×10 magnification (*A*) and at ×20 magnification (*B*). The inflammatory cells are a mixture of neutrophils and mononuclear cells, which are both intra-alveolar and within the alveolar walls (*C*). In contrast, the cav$^{+/+}$ mice (*D–F*) have lesser degrees of lung injury. The lungs demonstrate areas of patchy pulmonary consolidation (*D*) composed of intra-alveolar infiltrates of inflammatory cells (*E*), predominantly neutrophils and macrophages (*F*). Furthermore, there is prominent margination of both neutrophils and monocytes in large and medium-sized vasculature.

difference in lung architecture and morphology between the cav$^{-/-}$ and cav$^{+/+}$ mice at 6–8 weeks of age (data not shown). Although these findings contrast previous published results (16), it is probably due to the young age of the mice used in this study compared with the prior descriptions. Four hours after Pa infection, lung histopathology demonstrated recruitment of neutrophils into the lung parenchyma with airway inflammation and minimal alveolar filling. However, we did not observe any differences between the cav$^{-/-}$ or cav$^{+/+}$ groups (data not shown). However, by 16 h after infection, there was a striking difference with less lung injury in the cav −/− mice *versus* the cav+/+ mice (Fig. 2). Although both groups of mice displayed evidence of pneumonia with inflammatory cell infiltration, the amount of consolidation and number of inflammatory cells were markedly greater in the cav$^{+/+}$ controls. Although the lungs of the cav$^{+/+}$ mice revealed dense inflammatory infiltrates with areas of complete destruction of lung architecture, the cav$^{-/-}$ lungs showed fewer inflammatory cells, decreased lung injury, and preserved alveolar spaces. In order to quantify some of the histologic changes that were observed, we calculated the percentage of aerated and consolidated lungs in both groups of mice. Lungs from cav$^{-/-}$ mice had significantly less consolidation and a greater proportion of aerated lung compared with cav$^{+/+}$ mice. cav$^{-/-}$ mice were found to have 44% of the area consolidated compared with 55% consolidation of the lung from cav$^{+/+}$ mice (p = 0.012). The lower degree of histologic lung injury, lower BAL cell counts, and decreased levels of inflammatory cytokines parallel the significantly decreased bacterial burden within the lungs.

Pa Invasion Is Inhibited in Primary LECs Isolated from cav$^{-/-}$ Mice—We hypothesize that the ability of Pa to persist within the lung is due, at least in part, to their ability to invade the LECs and thereby avoid host defense mechanisms. cav$^{+/+}$ and cav$^{-/-}$ mice were intratracheally infected with GFP-expressing Pa. Confocal images of murine lungs showed a significant number of Pa that are co-localized with the alveolar epithelium (Fig. 3*A*) and appeared to be more common in the cav$^{+/+}$ compared with the cav$^{-/-}$ mice. In order to quantify the ability of Pa to invade LECs, we compared the ability of Pa to invade cultured primary tracheal epithelial cells *in vitro*. Isolation of primary murine tracheal epithelial cells from both the cav$^{-/-}$ and cav$^{+/+}$ mice was performed using established

FIGURE 1. **cav$^{-/-}$ mice are resistant to Pa pneumonia.** *A*, cav$^{-/-}$ mice (n = 20) and control cav$^{+/+}$ mice (n = 20) were intratracheally infected with 10^7 cfu of Pa (ATCC 27853) via direct intratracheal instillation. Although all cav$^{+/+}$ mice died within 48 h after infection, 50% of the cav$^{-/-}$ mice were able to survive and clear the Pa infection ($p < 0.0001$; hazard ratio 2.903; 95% confidence interval: 4.052–41.42). *B–E*, mice were sacrificed after 16 h to quantify the bacterial burden of Pa. cav$^{-/-}$ mice had significantly lower amounts of Pa within the lung (*B*; p = 0.0022) and BAL fluid (*C*; p = 0.0067). In contrast, there was no difference in the number of bacteria in the liver (*D*; p = 0.851) or spleen (*E*; p = 0.196). *F–I*, Cav$^{-/-}$ mice showed lower levels of inflammation in BAL fluid collected 16 h after infection. Both groups had >90% neutrophils in their BAL, but cav$^{-/-}$ mice had fewer total cells and a lower percentage of neutrophils compared with cav$^{+/+}$ mice (*F*; p = 0.160). The cav$^{-/-}$ mice also had lower levels of inflammatory cytokines in their BAL after Pa infection, including MIP-2 (*G*; p = 0.039), IL-1β (*H*; p = 0.0001), and tumor necrosis factor-α (*I*; p = 0.016).

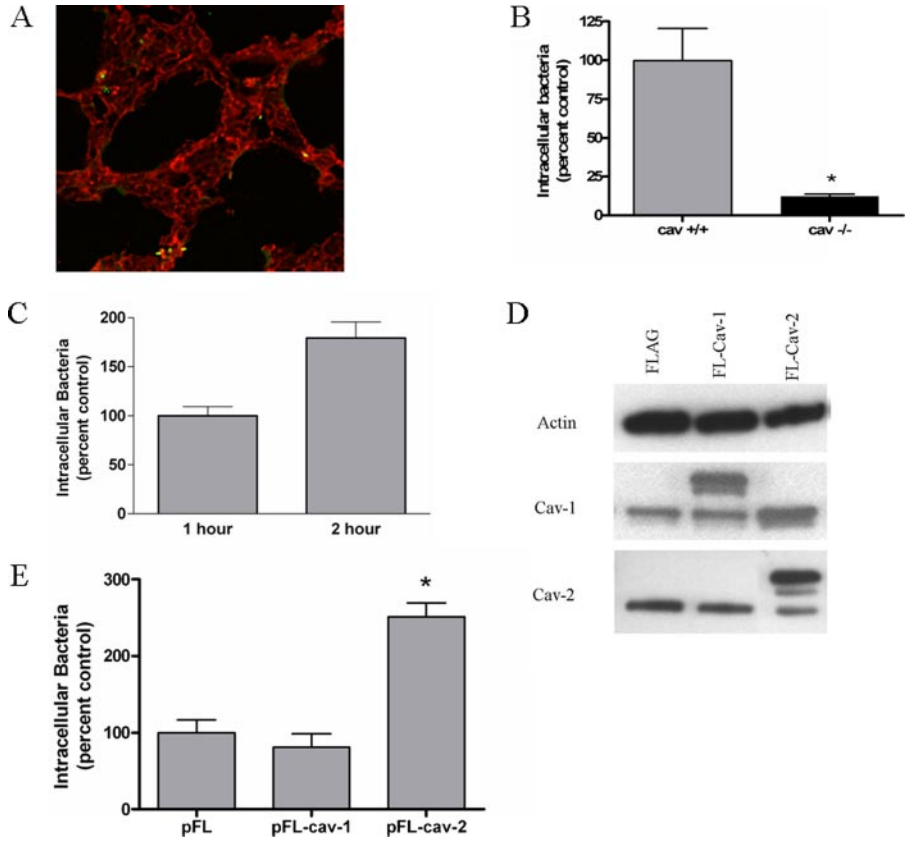

FIGURE 3. **Caveolin-2 regulates Pa invasion of LECs.** *A*, confocal images of murine lungs that were intratracheally infected with a GFP-expressing strain of Pa, ATCC 27853, show that a large number of Pa are co-localized with alveolar epithelial cells. Primary murine tracheal epithelial cells were isolated from both $cav^{+/+}$ and $cav^{-/-}$ mice in order to determine the role of caveolin expression on invasion of primary LECs. *B*, Pa invasion of primary tracheal epithelial cells was significantly inhibited in $cav^{-/-}$ cells ($p = 0.0040$). *C*, we quantified the number of intracellular Pa at 1 and 2 h after infection of primary tracheal epithelial cells. Pa was not only viable intracellularly but also was able to replicate within primary tracheal epithelial cells. *D*, MLE-12 cells overexpressing FLAG-tagged caveolin-1 (pFL-cav-1) or caveolin-2 (pFL-cav-2) were created to investigate the specific role of these proteins in the uptake of Pa. *E*, Pa uptake was not affected by the overexpression of caveolin-1; however, overexpression of caveolin-2 led to significant increases in the number of intracellular Pa ($p = 0.0032$).

techniques (27). The primary tracheal epithelial cells were infected with Pa for 1 h, and then a gentamicin protection assay was used to quantify the number of intracellular bacteria. $cav^{-/-}$ tracheal epithelial cells were resistant to invasion with a significantly decreased number of intracellular Pa compared with $cav^{+/+}$ controls (Fig. 3*B*, $p = 0.0040$). Pa has a greater ability to invade the $cav^{+/+}$ LECs, which we hypothesize can serve as an important virulence factor for the pathogen. Further studies of $cav^{+/+}$ tracheal epithelial cells confirmed not only that Pa is capable of invasion but also that it can survive and replicate intracellularly (Fig. 3*C*). In order to determine whether caveolin expression was required for uptake by alveolar macrophages, we isolated primary alveolar macrophages from both $cav^{+/+}$ and $cav^{-/-}$ mice and used a gentamicin protection assay to examine Pa uptake *in vitro*. Unlike LECs, we found that Pa uptake by alveolar macrophages was not inhibited in $cav^{-/-}$ mice (data not shown). Therefore, Pa invasion via lipid raft-mediated endocytosis by LECs allows survival of this important pathogen, and we believe it is a major determinant of the ability of the Pa to successfully colonize the lung.

Caveolin-2 Is a Major Determinant of the Ability of Pa to Invade LECs—Our previous work using RNA interference to inhibit both caveolin-1 and caveolin-2 expression has shown that caveolin expression is required for maximal invasion of a murine lung epithelial cell line (MLE-12) *in vitro* (6). In order to delineate the role of caveolin-1 *versus* caveolin-2 on Pa uptake, we created MLE-12 cells that overexpress FLAG-tagged caveolin-1 (pFL-cav-1) or caveolin-2 (pFL-cav-2) (Fig. 3*D*). pFL-cav-1 and pFL-cav-2 cells had no change in cell morphology, viability, or growth that was appreciated. Confocal microscopy confirmed that FLAG-tagged caveolin-1 and -2 was distributed normally within the cells, and sucrose gradient fractionation confirmed localization within the buoyant lipid raft fractions as expected (data not shown). The role of caveolin proteins in Pa invasion was examined by comparing uptake of Pa between stably transfected pFL-cav-1 and pFL-cav-2 cells compared with pFL vector-transfected controls. Overexpression of caveolin-1 had no effect on Pa invasion; however, overexpression of caveolin-2 significantly increased the number of intracellular Pa (Fig. 3*E*; $p = 0.0032$). We found no effect of caveolin overexpression on the invasion of *S. aureus* (data not shown). We have concluded that caveolin-2, and not caveolin-1, is the key protein that determines the ability of Pa to invade and persist within LECs. These studies have shown not only that caveolin-2 is required for Pa invasion but also that it can regulate this host endocytic pathway, thereby modulating Pa invasion of LECs. Although caveolin-1 knock-out mice lack expression of both caveolin-1 and caveolin-2, we hypothesize that the absence of caveolin-2 specifically is the major determinant of resistance we observed in the murine model by impairing bacterial invasion into LECs.

Overexpression of Caveolin-2 Can Increase the Lipid Raft-dependent Entry of Pa Due to Changes in the Caveolin-2 Signaling Pathways—Pretreatment with MCD (3 mM) disrupts lipid rafts and significantly inhibits Pa invasion *in vitro* (6). Pretreatment of pFL-cav-2 cells with MCD significantly inhibited Pa invasion (Fig. 4*A*; $p = 0.004$), confirming that the increased Pa invasion in pFL-cav-2 cells is due to increased lipid raft-mediated uptake and not a distinct lipid raft-independent pathway. We speculated that the effects of caveolin-2 were due to its role in cell signaling rather than any changes in the mechanical fluidity of the plasma membrane. Caveolin-2 is believed to play a role in several cell signaling pathways and has two known sites of tyrosine phosphorylation (19, 21). Pretreatment of pFL-cav-2 cells with the tyrosine kinase inhibitor genistein significantly decreased the number of intracellular Pa (Fig. 4*A*; $p = 0.021$).

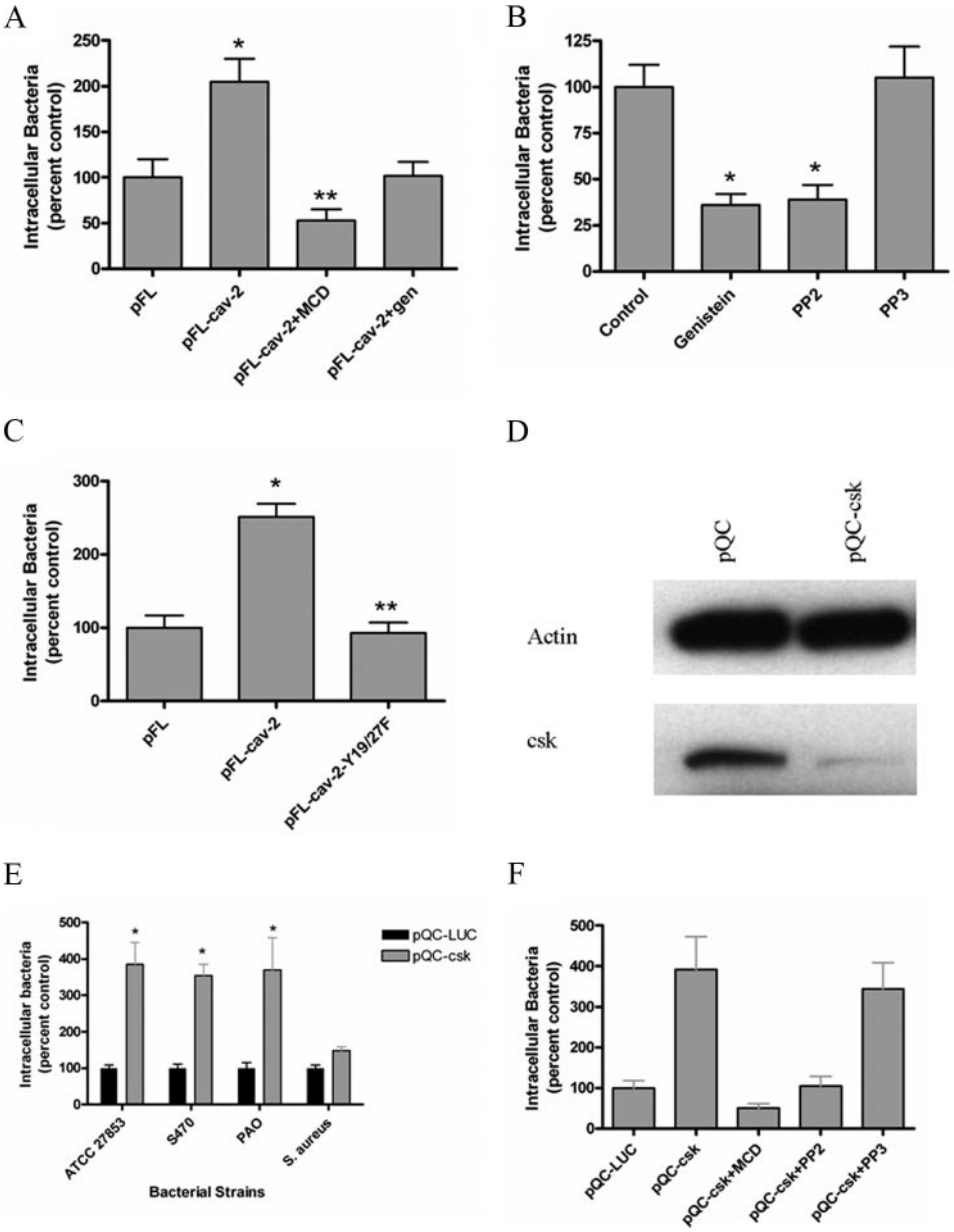

FIGURE 4. **Tyrosine phosphorylation of caveolin-2 regulates the lipid raft-mediated entry of Pa.** *A*, the increased uptake of Pa in pFL-cav-2 cells was inhibited with methyl-β-cyclodextrin ($p = 0.004$) and genistein ($p = 0.021$), indicating the dependence on both lipid raft integrity and tyrosine phosphorylation. *B*, MLE-12 cells were infected with Pa in the presence of different tyrosine kinase inhibitors to determine which specific class of tyrosine kinases are implicated. Pa invasion was inhibited by the nonspecific tyrosine kinase inhibitor genistein as well as the Src family kinase inhibitor, PP2 ($p = 0.0024$). PP3, an inhibitor of receptor-mediated tyrosine kinases, had no effect. *C*, in order to determine the significance of caveolin-2 phosphorylation, site-directed mutagenesis was used to change both sites of tyrosine phosphorylation, Tyr^{19} and Tyr^{27}, to phenylalanine (pFL-cav-2-Y19/27F). *D*, similar to the overexpression of wild type caveolin-2, pFL-cav-2-Y19/27F cells had increased expression of caveolin-2. However, pFL-cav-2-Y19/27F cells did not demonstrate any increased Pa invasion, showing that tyrosine phosphorylation of caveolin-2 is required for the increased uptake of Pa noted previously. *E*, pQC-Csk cells were created as stable transfections using RNA interference to decrease Csk expression and determine its role in Pa infection *in vitro*. Pa invasion of pQC-Csk cells was significantly increased for all three Pa strains tested: ATCC 27853, PAO, and S470. In contrast, the decreased expression of Csk had no effect on the uptake of *S. aureus*. *F*, Pa invasion of pQC-Csk cells is still inhibited by MCD, genistein, and PP2, reflecting that Pa invasion of pQC-Csk cells occurs through lipid raft-mediated endocytosis.

We next looked at the effect of different tyrosine kinase inhibitors on Pa uptake by LECs. We found that both genistein and the Src family kinase inhibitor PP2 significantly inhibited Pa invasion (Fig. 4*B*; $p = 0.0024$). On the other hand, PP3, which is known to inhibit receptor tyrosine kinases, such as epidermal growth factor receptor, had no effect on the number of intracellular Pa (Fig. 4*B*). Caveolin-2 has two known sites of tyrosine phosphorylation at positions 19 and 27 (19, 21). In order to confirm the role of tyrosine phosphorylation of caveolin-2, we used site-directed mutagenesis to change both of these sites to phenylalanine. Phosphorylation-incompetent caveolin-2 and wild type caveolin-2 were expressed in equal amounts according to Western blot and similar distribution when examined with confocal microscopy (data not shown). Although overexpression of wild type caveolin-2 (pFL-cav-2) increased Pa invasion, overexpression of the phosphorylation-incompetent mutant (pFL-cav-2-Y19/27F) was identical to controls and confirms that phosphorylation of caveolin-2 is required to increase Pa invasion (Fig. 4*C*). These studies confirmed that Pa uptake occurs via a host-regulated lipid raft dependent pathway controlled by caveolin-2 expression as well as tyrosine phosphorylation by Src family kinases.

Csk Negatively Regulates Caveolin-2-mediated Pa Invasion—To further evaluate the role of signaling pathways in modulating caveolin-dependent uptake of Pa, we examined the *in vitro* ability of different strains of Pa, including ATCC 27853 and PAO-1, to invade LECs in which the expression of Csk, a COOH terminus Src kinase, was inhibited (Fig. 4*D*). Using RNA interference, MLE-12 cells were stably transfected to create pQC-Csk cells with an approximately 90% decrease in Csk expression compared with pQC-LUC controls. Inhibition of Csk expression had no appreciable effect on cell morphology, viability, or growth (data not shown). Remarkably, we found that all of the Pa isolates tested exhibited a nearly 4-fold greater level of invasion into pQC-Csk cells compared with the pQC-LUC control LECs (Fig. 4*E*; $p = 0.0001$). In order to determine if the role of Csk in bacterial uptake was specific to Pa and lipid raft-mediated entry, we examined bacterial invasion with other bacteria that are known to invade via lipid raft-independent mechanisms, such as *Staphylococcus aureus*. This effect was specific to Pa, since we observed no difference in the bacterial invasion of *S.*

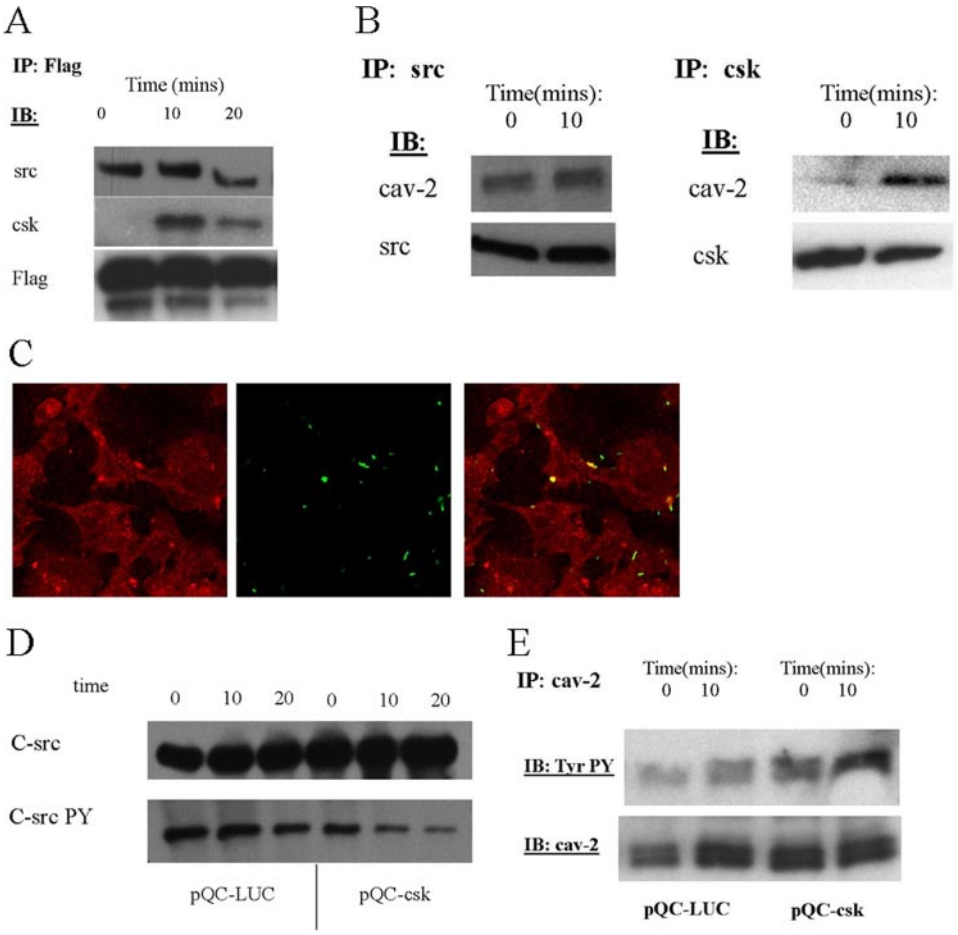

FIGURE 5. **Csk controls the phosphorylation of caveolin-2 via c-Src.** *A*, immunoprecipitation (*IP*) of FLAG-tagged caveolin-2 in pFL-Cav-2 cells revealed a strong association with c-Src before and after infection with Pa. In contrast, a transient association between caveolin-2 and Csk was only identified after infection with Pa. *B*, separate immunoprecipitation of both c-Src and Csk in wild type MLE-12 cells confirmed these same associations with native caveolin-2. c-Src was associated with caveolin-2 before and after infection, whereas Csk was only transiently associated with caveolin-2 after Pa infection. *C*, confocal microscopy staining shows that Csk (*red*) co-localizes with Pa (*green*) at the site of infection. Csk appears to accumulate on the plasma membrane at the site of entry but does not appear to encircle the intracellular bacteria. *D*, immunoprecipitation of c-Src before and after Pa infection was performed in order to determine the effect of Csk expression of c-Src during Pa infection. Immunoprecipitation of c-Src showed decreased phosphorylation of c-Src 529 in pQC-Csk cells compared with controls, reflecting an increase in the active form of c-Src. *E*, we used an immunoprecipitation of caveolin-2 to determine the indirect effects of Csk expression on caveolin-2 phosphorylation. Tyrosine phosphorylation of caveolin-2 was significantly increased at base line and after Pa infection as a result of the increased activity of c-Src in the pQC-Csk cells.

aureus in the pQC-Csk cells compared with controls (Fig. 4*E*). These findings suggest that inhibition of Csk expression was either initiating uptake of Pa via an alternative invasion mechanism or promoting increased lipid raft-mediated Pa entry. We hypothesized that Csk negatively regulates the lipid raft-mediated Pa invasion of LECs; therefore, its absence leads to increased numbers of intracellular Pa. To see if Csk inhibition was influencing the lipid raft-mediated entry of Pa, we examined the effects of MCD, a known inhibitor of lipid raft-mediated bacterial invasion. We found that the increased uptake of Pa found in the pQC-Csk cells is inhibited by treatment with MCD (Fig. 4*F*; $p = 0.003$). Since lipid raft-mediated uptake of Pa is also dependent on tyrosine phosphorylation, we examined the effects of different tyrosine kinase inhibitors on Pa invasion of pQC-Csk cells. The tyrosine kinase inhibitors genistein and PP2 significantly decreased the high levels of Pa uptake found in the pQC-Csk cells (Fig. 4*F*; $p = 0.002$), indicating that the mechanism of bacterial invasion in both pQC-Csk and pQC-LUC cells was dependent on lipid raft integrity and tyrosine phosphorylation. Therefore, we conclude that inactivation of Csk was not initiating a new mode of bacterial invasion, but rather, it was enhancing lipid raft-mediated Pa invasion of LECs.

Since Csk is known to regulate other members of the Src family kinases, we hypothesized that inhibition of Pa invasion in pQC-Csk cells may be due to the effects of Csk on other Src kinases that are directly responsible for the phosphorylation of caveolin-2. Therefore, we sought to identify the specific Src kinase that was interacting with caveolin-2 in lipid raft fractions. Five members of the Src family are predominantly located within lipid rafts: c-Src, Lyn, Fyn, Lck, and Csk (30). We overexpressed caveolin-2 using MLE-12 cells that were transfected with the FLAG-tagged caveolin-2 protein (pFL-cav-2), as described above. Immunoprecipitation (IP) was used to identify which members of the Src family associate with caveolin-2. We found no association between caveolin-2 and either Lyn, Fyn, or Lck (data not shown). On the other hand, IP of FLAG-cav-2 revealed a strong association with c-Src both before and after Pa infection (Fig. 5*A*), confirming that c-Src directly phosphorylates caveolin-2 (19, 21). We hypothesized that Csk inactivates c-Src and thereby indirectly regulates the phosphorylation of caveolin-2. Therefore, we examined the association of Csk with caveolin-2. Although we found no association between caveolin-2 and Csk at base line, appreciable amounts of Csk were associated with caveolin-2 after Pa infection (Fig. 5*A*). This transient association between Csk and caveolin-2 was observed at 10 min after infection and was no longer present after 30 min. Indeed, the association of caveolin-2 with c-Src and Csk was confirmed using an IP using either Src and Csk and then blotting for caveolin-2. Although c-Src again showed a constant association with caveolin-2 (Fig. 5*B*), Csk was associated with caveolin-2 only after Pa infection (Fig. 5*B*). The immunoprecipitation of these Src family kinases with caveolin-2 during Pa infection helps elucidate the important roles played by Csk, c-Src, and caveolin-2 in regulating the lipid raft-mediated uptake of bacteria.

To further demonstrate the critical role of Csk in negatively regulating Pa uptake, we examined the Pa-infected LECs to see

if there was any co-association of Pa and Csk. MLE-12 cells were infected with GFP-expressing Pa *in vitro*. Confocal microscopy consistently showed that the localization of Csk expression significantly changed after Pa infection. Csk concentrates at the site of Pa infection on the plasma membrane and co-localizes with fluorescently labeled Pa (Fig. 5*C*).

Since Csk is known to phosphorylate the inactivating site of c-Src, Tyr(P)^{529}, we examined if this was the case in Pa-infected LECs. An IP of c-Src confirmed that phosphorylation of Src Tyr^{529} was inhibited in the pQC-Csk cells both before and after infection with Pa (Fig. 5*D*). Since increased phosphorylation of Src Tyr^{529} inhibits its activity, we next sought to determine the role of Csk on caveolin-2 phosphorylation. An IP of caveolin-2 showed that pQC-Csk cells have increased phosphorylation of caveolin-2 at base line; however, there is a more significant increase in phosphorylation 10 min after Pa infection (Fig. 5*E*). Therefore, Csk not only regulates the inhibitory phosphorylation of c-Src but also indirectly controls caveolin-2 phosphorylation after Pa infection. Cumulatively, these data reveal that Csk plays an important role in regulation of lipid raft-mediated Pa invasion by manipulating the phosphorylation of caveolin-2. The ability of Csk to inhibit phosphorylation of caveolin-2 and decrease Pa invasion of LEC appears to be a novel host defense mechanism that is triggered after Pa infection.

DISCUSSION

The role of caveolin proteins and lipid rafts in the pathogenesis of bacterial infections is just beginning to be understood. We observed a striking difference in lethality of Pa infection between cav$^{-/-}$ and cav$^{+/+}$ mice. The resistance to Pa infection was associated with a markedly decreased bacterial burden but no difference in the systemic dissemination of Pa. These data suggest that the mice succumbed to overwhelming Pa pneumonia and demonstrate the unique role of caveolin proteins within the lung in the pathogenesis of Pa infection. The significance of Pa invasion of LECs during the pathogenesis of pneumonia has been controversial. For the first time, we have shown that caveolin expression enables Pa invasion and bacterial replication, which increases mortality in an acute bacterial pneumonia model. We hypothesized that invasion via lipid raft-mediated uptake is an important virulence factor for pathogens that allows survival within a protected intracellular niche and avoidance of host defense mechanisms. Bacteria can develop novel virulence factors as they evolve ways to avoid host defense mechanisms. Pa is part of a growing list of pathogens that have evolved ways to co-opt lipid raft-mediated endocytosis as a means of invading host cells (10, 11), and the resistance of the caveolin-deficient mice demonstrates the evolutionary benefit that invasion can provide to pathogens.

Previous work has shown that caveolin-1 is a negative regulator of cell signaling pathways and that caveolin-1 deficiency increases production of proinflammatory cytokines (31). However, our studies at 16 h showed significantly lower levels of inflammatory cytokines in the BAL fluid and less neutrophil recruitment within the lung. These results were initially surprising, since the i*n vitro* studies have shown that alveolar macrophages from cav$^{-/-}$ mice produce higher levels of inflammatory cytokines in response to lipopolysaccharide (31). The contrasting results observed *in vivo* with lower levels of proinflammatory cytokines in the cav$^{-/-}$ mice are most likely due to the lower bacterial burden present in cav$^{-/-}$ mice. The improved clearance of Pa in the caveolin-deficient mice led to significantly lower bacterial burdens by 16 h, decreased histologic measures of lung injury, lower levels of inflammatory cytokines, and markedly improved survival. The resistance of the cav$^{-/-}$ mice to Pa pneumonia contrasts with the previous work showing that cav$^{-/-}$ mice are more susceptible to intraperitoneal infection with salmonella and have a higher mortality (32). Several possible reasons exist for these different observations. Unlike Pa, salmonella does not require lipid rafts for invasion of host epithelial cells, which is inhibited in the cav$^{-/-}$ mice. In addition, the salmonella-infected mice died from overwhelming sepsis and an exaggerated inflammatory response, whereas our Pa-infected mice appeared to die from uncontrolled pneumonia and respiratory failure.

Caveolin-1 knock-out mice are deficient in not only caveolin-1 but also caveolin-2, due to the requirement of caveolin-1 to transport caveolin-2 to the cell surface (33). Our *in vitro* data strongly suggest that the phenotype of the caveolin-deficient mice is due to the absence of caveolin-2 and not caveolin-1. We have shown that only the overexpression of caveolin-2 and not caveolin-1 increases the Pa uptake by LECs. In our model, caveolin-2 appears to be the major player, whereas caveolin-1 predominantly functions as a chaperone protein that is required to deliver caveolin-2 to the plasma membrane. In addition, Pa invasion of LEC requires tyrosine phosphorylation of caveolin-2 by Src family kinases. It is not yet known how caveolin-2 phosphorylation is able to regulate lipid raft-mediated endocytosis. We have speculated that phosphorylated caveolin-2 interacts with cytoskeletal proteins, such as actin, and mediates the formation of the lipid raft-enriched platforms that occur at the site of bacterial attachment and are required for bacterial invasion. These data strongly implicate caveolin-2 as a novel signaling molecule that regulates not only lipid raft-mediated endocytosis but also host susceptibility to a common bacterial infection and common cause of death for hospitalized patients and immunocompromised hosts.

The ability to successfully invade host cells represents a powerful advantage to an infectious agent. Not only does it provide the pathogen with an intracellular niche for growth, but it protects the pathogen from the clearance actions of mucosal flow and phagocytic cells. Not surprisingly, studies have focused almost exclusively on the various mechanisms pathogens utilize to gain entry into host cells. The notion that host cells may have evolved mechanisms to actively resist the entry of the pathogens has not been investigated. Recently, however, Song *et al.* (34) reported that bladder epithelial cells are intrinsically able to resist the entry of uropathogenic *Escherichia coli*. Furthermore, this activity was initiated by the lipopolysaccharide ligand, TLR4, and a secondary messenger cAMP (34). Our studies have revealed that LECs are also capable of actively resisting the entry of Pa and that the mechanism of resistance involves Csk. This kinase was found to counteract the Pa-mediated phosphorylation of caveolin-2 by inactivating c-Src. In the absence of Csk, the unregulated phosphorylation of caveolin-2 increases, and lipid raft-dependent internalization of Pa

progresses undeterred, resulting in 4-fold increases in the number of intracellular Pa. What molecules signal Csk after Pa infection is currently not known, but it is intriguing that a prominent secondary messenger known to activate Csk is also cAMP (35).

Understanding the role of host cell signaling pathways, including caveolin-2 and Csk, has implications that may lead to advances in the treatment of patients with Pa pneumonia. Although a large percentage of hospitalized patients develop colonization with this common pathogen, only a subset develop clinical infection with varying severity of bacterial pneumonia. We speculate that genetic polymorphisms in genes that regulate the lipid raft-mediated uptake of Pa may contribute to the susceptibility to Pa pneumonia in addition to the typical clinical risk factors. Another implication of a better understanding of these new host defense mechanisms against Pa infection could be the development of new treatment strategies designed to augment host innate defense mechanisms, such as Csk. Traditional therapies for bacterial infections have relied on antibiotics that target bacteria and have been limited by the rapid development of resistance. Novel therapies aimed at augmenting these natural host defense mechanisms may serve as important adjunctive therapies to traditional antibiotics or even prophylactic strategies in high risk patients.

REFERENCES

1. Fagon, J. Y., Chastre, J., Domart, Y., Trouillet, J. L., and Gibert, C. (1996) *Clin. Infect. Dis.* **23,** 538–542
2. Dunn, M., and Wunderink, R. G. (1995) *Clin. Chest Med.* **16,** 95–109
3. Driscoll, J. A., Brody, S. L., and Kollef, M. H. (2007) *Drugs* **67,** 351–368
4. Crouch Brewer, S., Wunderink, R. G., Jones, C. B., and Leeper, K. V., Jr. (1996) *Chest* **109,** 1019–1029
5. Chastre, J., and Fagon, J. Y. (2002) *Am. J. Respir. Crit. Care Med.* **165,** 867–903
6. Zaas, D. W., Duncan, M. J., Li, G., Wright, J. R., and Abraham, S. N. (2005) *J. Biol. Chem.* **280,** 4864–4872
7. Grassme, H., Jendrossek, V., Riehle, A., von Kurthy, G., Berger, J., Schwarz, H., Weller, M., Kolesnick, R., and Gulbins, E. (2003) *Nat. Med.* **9,** 322–330
8. Garcia-Medina, R., Dunne, W. M., Singh, P. K., and Brody, S. L. (2005) *Infect. Immun.* **73,** 8298–8305
9. Anderson, R. G. (1998) *Annu. Rev. Biochem.* **67,** 199–225
10. Zaas, D. W., Duncan, M., Rae Wright, J., and Abraham, S. N. (2005) *Biochim. Biophys. Acta* **1746,** 305–313
11. Shin, J. S., and Abraham, S. N. (2001) *Microbes Infect.* **3,** 755–761
12. Parton, R. G., and Richards, A. A. (2003) *Traffic* **4,** 724–738
13. Parolini, I., Sargiacomo, M., Galbiati, F., Rizzo, G., Grignani, F., Engelman, J. A., Okamoto, T., Ikezu, T., Scherer, P. E., Mora, R., Rodriguez-Boulan, E., Peschle, C., and Lisanti, M. P. (1999) *J. Biol. Chem.* **274,** 25718–25725
14. Mora, R., Bonilha, V. L., Marmorstein, A., Scherer, P. E., Brown, D., Lisanti, M. P., and Rodriguez-Boulan, E. (1999) *J. Biol. Chem.* **274,** 25708–25717
15. Scherer, P. E., Okamoto, T., Chun, M., Nishimoto, I., Lodish, H. F., and Lisanti, M. P. (1996) *Proc. Natl. Acad. Sci. U. S. A.* **93,** 131–135
16. Razani, B., Engelman, J. A., Wang, X. B., Schubert, W., Zhang, X. L., Marks, C. B., Macaluso, F., Russell, R. G., Li, M., Pestell, R. G., Di Vizio, D., Hou, H., Jr., Kneitz, B., Lagaud, G., Christ, G. J., Edelmann, W., and Lisanti, M. P. (2001) *J. Biol. Chem.* **276,** 38121–38138
17. Williams, T. M., and Lisanti, M. P. (2004) *Ann. Med.* **36,** 584–595
18. Schlegel, A., and Lisanti, M. P. (2001) *Cytokine Growth Factor Rev.* **12,** 41–51
19. Wang, X. B., Lee, H., Capozza, F., Marmon, S., Sotgia, F., Brooks, J. W., Campos-Gonzalez, R., and Lisanti, M. P. (2004) *Biochemistry* **43,** 13694–13706
20. Lee, H., Volonte, D., Galbiati, F., Iyengar, P., Lublin, D. M., Bregman, D. B., Wilson, M. T., Campos-Gonzalez, R., Bouzahzah, B., Pestell, R. G., Scherer, P. E., and Lisanti, M. P. (2000) *Mol. Endocrinol.* **14,** 1750–1775
21. Lee, H., Park, D. S., Wang, X. B., Scherer, P. E., Schwartz, P. E., and Lisanti, M. P. (2002) *J. Biol. Chem.* **277,** 34556–34567
22. Kim, H. P., Wang, X., Nakao, A., Kim, S. I., Murase, N., Choi, M. E., Ryter, S. W., and Choi, A. M. (2005) *Proc. Natl. Acad. Sci. U. S. A.* **102,** 11319–11324
23. Wang, X. M., Zhang, Y., Kim, H. P., Zhou, Z., Feghali-Bostwick, C. A., Liu, F., Ifedigbo, E., Xu, X., Oury, T. D., Kaminski, N., and Choi, A. M. (2006) *J. Exp. Med.* **203,** 2895–2906
24. Razani, B., Wang, X. B., Engelman, J. A., Battista, M., Lagaud, G., Zhang, X. L., Kneitz, B., Hou, H., Jr., Christ, G. J., Edelmann, W., and Lisanti, M. P. (2002) *Mol. Cell Biol.* **22,** 2329–2344
25. Bloemberg, G. V., O'Toole, G. A., Lugtenberg, B. J., and Kolter, R. (1997) *Appl. Environ. Microbiol.* **63,** 4543–4551
26. Mercer, A. A., and Loutit, J. S. (1979) *J. Bacteriol.* **140,** 37–42
27. Davidson, D. J., Gray, M. A., Kilanowski, F. M., Tarran, R., Randell, S. H., Sheppard, D. N., Argent, B. E., and Dorin, J. R. (2004) *J. Cyst. Fibros.* **3,** Suppl. 2, 59–62
28. You, Y., Richer, E. J., Huang, T., and Brody, S. L. (2002) *Am. J. Physiol.* **283,** L1315–L1321
29. Restrepo, C. I., Dong, Q., Savov, J., Mariencheck, W. I., and Wright, J. R. (1999) *Am. J. Respir. Cell Mol. Biol.* **21,** 576–585
30. Li, S., Seitz, R., and Lisanti, M. P. (1996) *J. Biol. Chem.* **271,** 3863–3868
31. Garrean, S., Gao, X. P., Brovkovych, V., Shimizu, J., Zhao, Y. Y., Vogel, S. M., and Malik, A. B. (2006) *J. Immunol.* **177,** 4853–4860
32. Medina, F. A., de Almeida, C. J., Dew, E., Li, J., Bonuccelli, G., Williams, T. M., Cohen, A. W., Pestell, R. G., Frank, P. G., Tanowitz, H. B., and Lisanti, M. P. (2006) *Infect. Immun.* **74,** 6665–6674
33. Li, S., Galbiati, F., Volonte, D., Sargiacomo, M., Engelman, J. A., Das, K., Scherer, P. E., and Lisanti, M. P. (1998) *FEBS Lett.* **434,** 127–134
34. Song, J., Bishop, B. L., Li, G., Duncan, M. J., and Abraham, S. N. (2007) *Cell Host Microbe* **1,** 287–298
35. Vang, T., Abrahamsen, H., Myklebust, S., Horejsi, V., and Tasken, K. (2003) *J. Biol. Chem.* **278,** 17597–17600